ISSN: 2455-1848
International Journal of Innovative Research & Growth
A Peer Reviewed & Referred International Journal
Volume-9 Issue-7 May-2020
Impact Factor-3.0
www.ijirg.com, editor@ijirg.com

# Indian Ber & Jamun Seeds Mediated Preparation of $Zn^{2+}$ Doped MgO Nanoparticles and Study Its Structural and Optical Properties

**[1]Preetam Singh Gour, [2]Shikha Munjal, [3]Pankaj Srivastava, [4]Nitin P. Singh**
[1,3,4]Department of Physics, School of Basic Sciences, Jaipur National University, Jaipur, Rajasthan, India
[2]Department of Chemistry, Dronacharya Senior Secondary School, Mubarikpur, Koshli, Rewari, Haryana, India
Email- pankajsrivastava0811@gmail.com, singhpreetamsingh@gmail.com

***Abstract***
*Nanotechnology is currently a flourishing field provides a novel way to fabricate nanoparticles exploring biological sources. The present study is devoted to doping $Zn^{2+}$ in MgO nanoparticles. Synthesized via green synthesis method using Indian ber seed and Jamun seed extract, were calcined at 450˚C to get the $Zn^{2+}$ doped MgO nanoparticles. The crystalline nature and particle size of the samples were characterized by X-ray diffraction analysis (XRD). The presence of the functional group in the sample is investigated using FTIR. The morphology of samples was studied by scanning electron microscope (SEM) and the presence of Zn in the sample was confirmed by energy dispersive X-ray analysis (EDX). The optical band gap of the $Zn^{2+}$ doped MgO nanoparticles sample was studied by UV-Vis spectroscopy. Optical band gap energy was found 3.10 eV with $Zn^{2+}$ doped MgO. SEM image of Zn2+ doped MgO particles was obtained morphology of $Zn^{2+}$ doped MgO structures. Most of these structures have diameters of 20-70 nm. The optical properties of the samples were investigated using photoluminescence spectroscopy (PL) analysis to obtain excitation and emission spectra of the samples and absorption near 335 nm and emission bands attributed to defects were observed in the PL spectra. Energy dispersive X-ray spectroscopy (EDAX) define the presence of elemental metal signal (magnesium, zinc and oxygen) was confirmed.*
**Keywords: -** Green Synthesis, Optical Properties, Nanomaterials.

## 1- INTRODUCTION

Magnesium oxide (MgO) nanoparticles with large surface area have been investigated comprehensively in various applications, such as in catalysts, catalyst support, hazardous waste treatment, antimicrobial materials, refractory materials, destructive adsorbent for a large number of pollutants, and superconductor materials [1-3]. Furthermore, doping is an important parameter used for nanoparticles due to the reformation of physicochemical properties of metal oxide, which has broad applications, namely in optoelectronics, dilute magnetic semiconductors, and photo detectors [4]. In addition, the wide range of applications can be affected by the particle size and crystal morphology of particles determined by scientists to concentrate on the synthesis of Zn2+ doped MgO nanoparticles. Different synthesis methods have been expressed, including thermal evaporation [5], flame spray pyrolysis [6], the sol-gel technique [7], chemical vapor deposition [8], hydrothermal [9], the auto combustion method [10], and the microwave-induced combustion process [3]. Nevertheless, some of these preparation methods are expensive and complicated processes. Moreover, the use of environmentally cancerous chemicals and organic solvents, which are poisonous, leads to large quantities of wastes inserted into water

sources and environments [5-10]. To solve these problems, a simple and viable alternative to chemical and physical methods, namely a green method. Plant mediated synthesis is purely a green synthetic route and are considered better candidates among the different biological entities as they provide clean, ecofriendly, cost effective, safe, conveniently utilizable and beneficial way to the synthesis of metal NPs for the large scale production. Many plants are reported to facilitate the formation of $Zn^{2+}$ doped MgO NPs and their potential applications. The amount of accumulation of NPs varies with reduction potential of ions and the reducing capacity of plant depends on the presence of various polyphenols and other heterocyclic compounds [11-12] . In this paper, an attempt was made to synthesize $Zn^{2+}$ doped MgO nanoparticles using Indian ber seed and Jamun seed extract, and it is an attractive process to achieve good homogeneity and composition control. Analysis of the $Zn^{2+}$ doped MgO nanoparticles was carried out using X-ray diffraction, field emission scanning electron microscopy, and electrical properties of the nanoparticles were investigated using UV–visible spectroscopy and optical properties of the nanoparticles were investigated using PL spectroscopy.

## 2- RESEARCH METHODOLOGY & RESULTS

### 2.1- MATERIALS SYNTHESIS

The synthesis of $Zn^{+2}$ doped MgO nanoparticles contains two steps as shown figure [1 & 2]-

- Preparation of plant extract of syzygium cumini seeds and ziziphus mauritiana seeds.
- Green synthesis of $Zn^{+2}$ doped MgO NPs.

#### 2.1.1- Preparation of Plant Extracts of Indian Ber & Jamun Seeds

The seeds of Indian ber & jamun were collected from the Jagatpura, Jaipur [Table 1]. The collected seeds were washed 3-4 times with distilled water to remove dust particles and impurities. Then, they were dried in hot air oven at 150°C for 1 hour and crushed it into powdered form. About 3g crushed form of Indian ber seeds and 3g of jamun seeds was weighed into a 250 ml beaker containing 100ml of de-ionised water and 50ml ethanol. Then, the solution was boiled for about 30 mins at 80°C. The solution was allowed to settle down for overnight and was filtered with Whatman filter paper. Hence, store the extract solution for the further analysis of nanoparticles as shown in Fig [1{a,b,c,d,e}].

**Table .1** List of plant species used for the green synthesis of $Zn^{2+}$ doped MgO NPs

| Plant Species | Common Name | Family | Type |
|---|---|---|---|
| Syzygium cumini (S. cumini) | Jamun seed | Myrtaceae | Plants (seed) |
| Ziziphus mauritiana (Z. mauritiana) | Ber seed | Rhamnaceae | Plants (seed) |

**Fig.1.(a)** Ziziphus mauritiana seed

**Fig.1.(b)** Syzygium cumini seed

**Fig.1.(c)** Ziziphus Mauritiana Powder

**Fig.1.(d)** Syzygium cumini powder

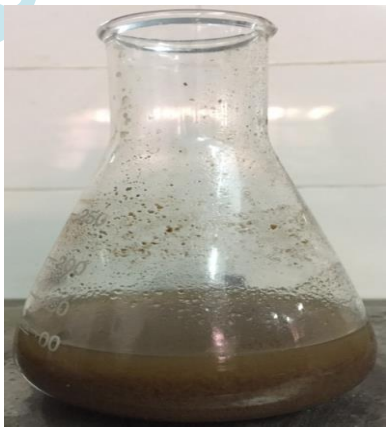

**Fig.1.(e)** Plant extract

### 2.1.2- Green Synthesis of $Zn^{+2}$ Doped MgO Nanoparticles

The $Zn^{+2}$ doped MgO nanoparticles were synthesized by adding 5g of magnesium chloride ($MgCl_2$), 5g of zinc chloride ($ZnCl_2$) and 50ml plant extract in 250 ml of distilled water. The pH of the solution was adjusted by adding the concentrated HCl solution. The resulting acidic solution was heated at 80°C for 2 hrs under constant stirring by using magnetic stirrer. After two hours of continuous stirring, the solution was allowed to settle down for overnight. Then, the solution was centrifuged for 12 mins at 15000 – 20000 rpm. The resulting precipitates were filtered, washed repeatedly for 2-3 times with distilled water and absolute ethanol. Finally, the separately nanoparticles were dried at room temperature and calcinated at 450°C for 2.5 hours in muffle furnace. The milky white nanoparticles were prepared as shown in fig [2{a,b,c,d}] and grinned by mortar pestle to get the finest particles for the further characterizations.

**Fig.2.(a)** Intermediate solution


**Fig.2.(b)** after centrifuge

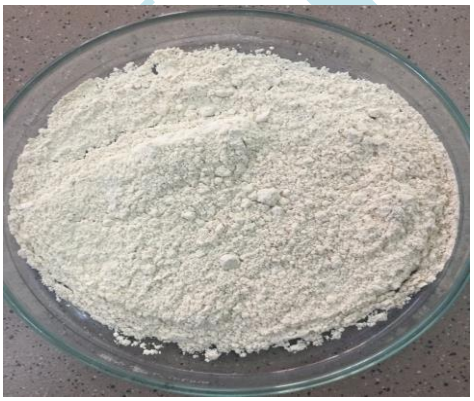

**Fig.2.(c)** Before calcination NPs

**Fig.2.(d)** after calcinations NPs

## 2.2- MATERIAL CHARACTERISTICS

### 2.2.1- Structural Properties

#### 2.2.1.1- Fourier Transform Infra Red Spectroscopy (FTIR)

Fourier transformation infrared spectroscopy (FTIR) of $Zn^{+2}$ doped MgO Nanoparticles was recorded from Perkin Elmer spectrum version 10.4.00 (4000-400 $cm^{-1}$). The IR analysis is used to determine the functional groups present in synthesized material and the way by which oxygen is bound to the metal ions [Table 2]. In graph Fig [3.1], the broad band of 3000 - 3500 $cm^{-1}$ is attributed to OH stretching vibration and the different capping agents present in plant extract which get merged with the surface of nanoparticles where as the peak at 1444.33 $cm^{-1}$ corresponds to the bending vibration of OH bond and Mg – OH stretching vibrations. The absorption peak at 1622.2 $cm^{-1}$ is due to the stretching and bending vibration of water [14-16]. The peak at 881.38 $cm^{-1}$, 530.27 $cm^{-1}$, 436.02 $cm^{-1}$ is attributed to the vibration of Zinc oxide or magnesiumoxide [17-19].

**Table-2** Functional group in FTIR spectra

| Functional group | Vibration | Absorption | Intensity |
|---|---|---|---|
| $Mg(OH)_2$ | Stretch, H-bond | 3439.92 | Strong, Broad |
| $-OH(H_2O)$ | Stretch | 1622.2 | Variable |
| Mg-OH | Stretch | 1444.33 | Medium |
| MgO | Stretch | 530.27 | Strong |

. .

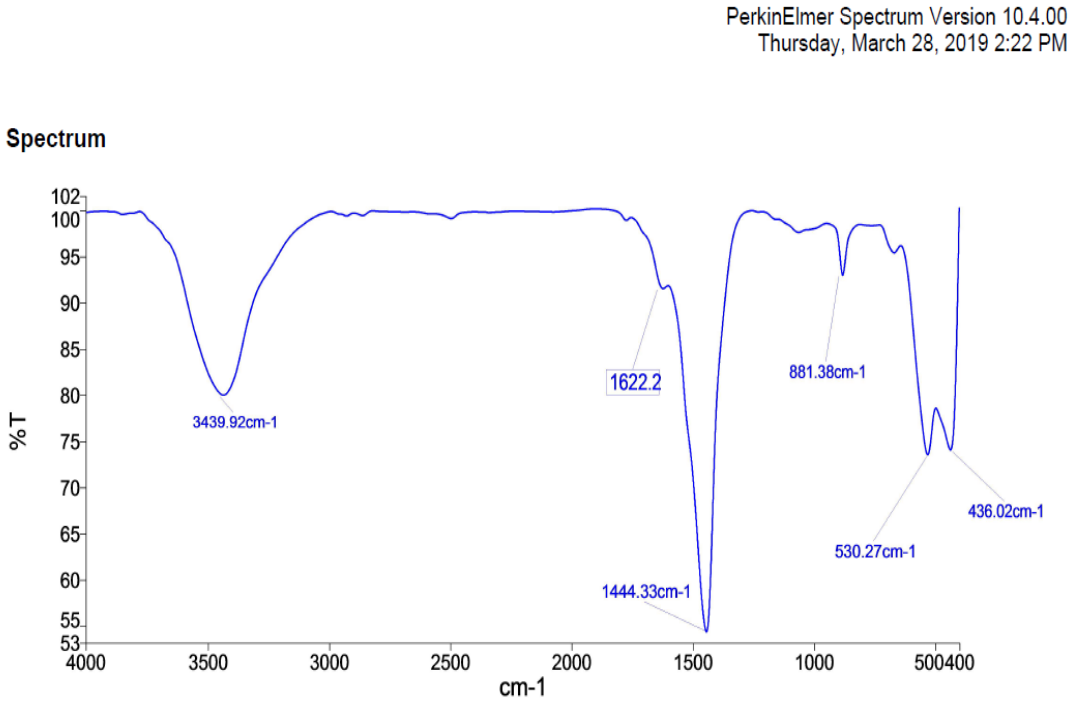


**3.1** FT-IR spectra of $Zn^{2+}$ doped MgO nanoparticles

**2.2.1.2- XRD Analysis**

X-ray diffraction (XRD) is the technique that reveals structural information. Materials researchers use XRD to analyze a wide range of materials, from powder X-ray diffraction to solids, thin films and nanomaterials. The characteristic x-ray diffraction pattern generated in a typical XRD analysis provides a unique "fingerprint" of the crystals present in the sample. When properly interpreted, by comparison with standard reference patterns and measurements, this fingerprint allows identification of the crystalline form. The synthesized $Zn^{2+}$ doped MgO NPs were analysis using Bruker AXS (Diffraktometer D8, Germany) in Bansthali University.

The X- Ray diffraction analysis investigated the phase and crystal structure of sample. The X – Ray diffraction peaks at 2θ = 27.15°, 31.57°, 34.32°, 36.12°, 42.57°, 45.20°, 47.47°, 56.54°, 62.76°, 67.78°, 74.95°, 83.80° correspond to the crystal plane of (111), (200), (210), (220), (221), (311), (211), (222), (321), (400), (421) and (430) of crystalline $Zn^{+2}$ doped MgO nanoparticles, respectively [ Fig 3.2]. The peak 31.57° correspond to the crystal plane (200) is the most intense peak among all the peaks. The diffraction peaks related to the impurities were not observed in the XRD analysis. The sharp and intense peak indicates the highly crystalline nature of $zn^{+2}$ doped MgO nanoparticles. The average crystalline size of $Zn^{+2}$ doped MgO nanoparticles were calculated from higher intense peak using Debye Scherrer's equation [13]

$$D = K\lambda / \beta Cos\theta$$

Where D is the crystalline size of the nanoparticles, λ is the wavelength of X – rays used in XRD analysis, β is the full width at half maximum of diffraction peak, K is the Scherrer's constant with a value of 0.9 to 1, and θ is the Bragg's angle. The calculated particle size of $Zn^{+2}$ doped MgO nanoparticles is 44 nm.

$$D = 0.9\lambda / \beta Cos\theta$$

The average crystalline size was calculated using Debye Scherrer's equation is 44.75 nm. The starin value based on diffraction peak broadening is –

$$\epsilon = \beta \, Cos \, (\theta/4)$$

$$\epsilon = .2871$$

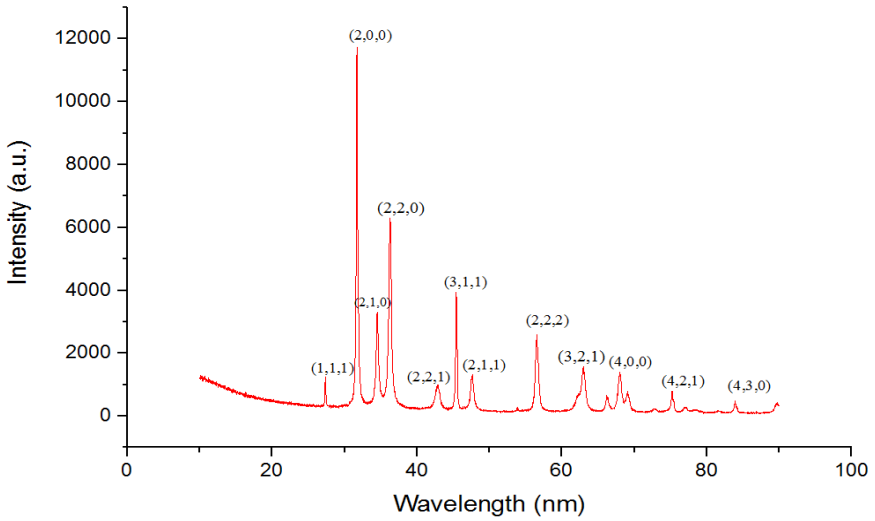


**Fig.3.2** XRD pattern of $Zn^{2+}$ doped MgO NPs powder.

### 2.2.1.3- FE-SEM Analysis

A scanning electron microscope (SEM) is a type of electron microscope that produces images of a sample by scanning the surface with a focused beam of electrons. The electrons interact with atoms in the sample, producing various signals that contain information about the surface topography and composition of the sample Figure [3.3 (a-d)]. Synthesized $Zn^{2+}$ doped MgO NPs were analysis using Nova Nano SEM 450 in MNIT, Jaipur.

The particle size of the $Zn^{2+}$ doped MgO is 44.75 nm. The synthesized nanoparticles showed some agglomeration due to the polarity and electrostatic attraction of $Zn^{2+}$ doped MgO nanoparticles. As the concentration of dopant increases, agglomeration increases and the particles size increases.. The conductivity of the $Zn^{2+}$ doped MgO sample is very low, the surface charge of the $Zn^{2+}$ doped MgO sample accumulates and the surface discharge occurs with increasing resolution of the image. The clear SEM image of Zn2+ doped MgO particles was obtained after about 1, 20,000 times resolution. The SEM image revealed different sizes for synthesized structures, too. Most of these structures have diameters of 20-70 nm [20-21].

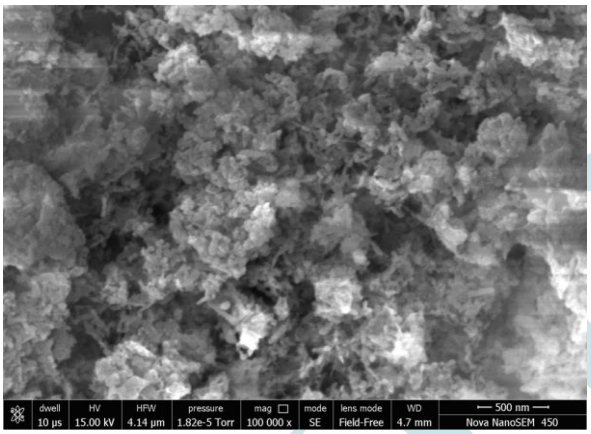


**Fig.3.3 (a)** FE-SEM images of $Zn^{2+}$ doped MgO nanoparticles

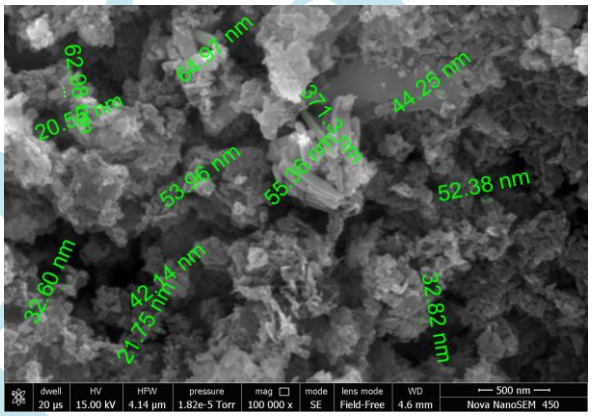


**Fig.3.3 (b)** FE-SEM images of $Zn^{2+}$ doped

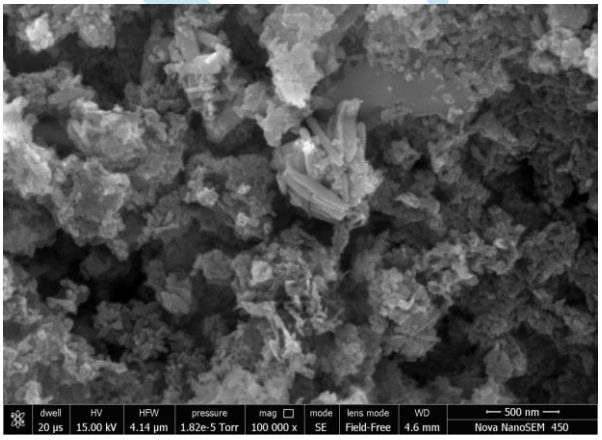


**Fig.3.3(c)** FE-SEM images of $Zn^{2+}$ doped MgO nanoparticles

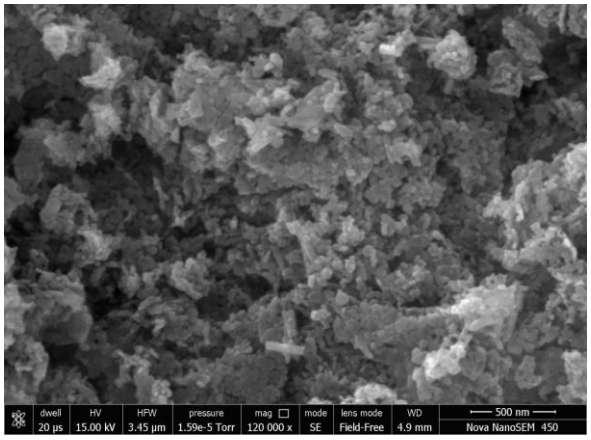


**Fig.3.3 (d)** FE-SEM images of $Zn^{2+}$ doped MgO nanoparticles

### 2.2.1.4- EDS Analysis

Energy-dispersive X-ray spectroscopy (EDS), sometimes called energy dispersive X-ray analysis (EDXA) or energy dispersive X-ray microanalysis (EDXMA), is an analytical technique used for the elemental analysis or chemical microanalysis technique used in conjunction with scanning electron microscopy (SEM) [3.4]. Synthesized $Zn^{2+}$ doped MgO NPs were analysis using Nova NanoSEM 450 in MNIT, Jaipur.

Energy dispersive X-ray spectroscopy (EDAX) was employed to establish the element identity of the observed particles in Figure 3.4. In the analysis by energy dispersive X-ray spectroscopy (EDX) of the $Zn^{2+}$ doped MgO nanoparticles, the presence of elemental metal signal (magnesium, zinc and oxygen) was confirmed.

The EDX spectral analysis reveals the presence of oxygen, chlorine, magnesium and zinc in the synthesized nanoparticles by which the presence of zinc and magnesium was confirmed [Table 3]. The appearance of peak of Cl and O is due to presence of biological moieties of plant at the surface of Zn supported MgO nanostructure.

**Table-3** Presence of element in $Zn^{2+}$ doped MgO NPs.

| Element | Atomic Number | unn. C [wt.%] | norm. C [wt.%] | Atom. C [at.%] |
|---|---|---|---|---|
| Zn | 30 | 43.94 | 53.99 | 26.56 |
| O | 8 | 19.40 | 23.84 | 47.93 |
| Mg | 12 | 10.57 | 12.99 | 17.19 |
| Cl | 17 | 7.47 | 9.18 | 8.32 |
| | Total | 81.38 | 100 | 100 |

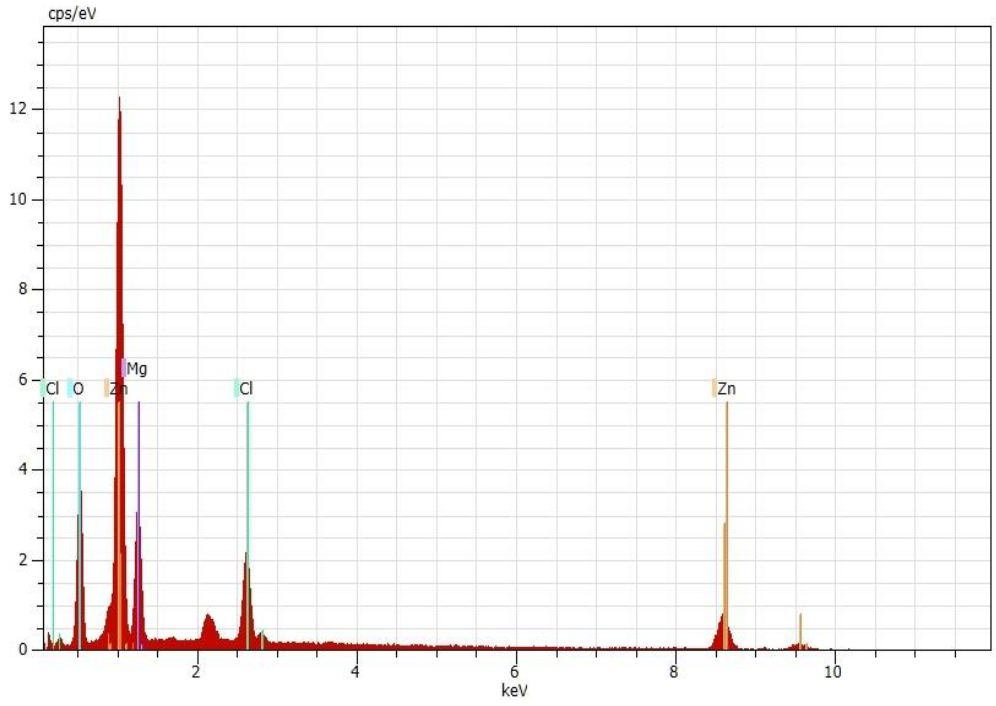


**Fig.3.4** EDS of the Zn2+ doped MgO nanoparticles

### 2.2.2- Optical Properties

#### 2.2.2.1- UV-VIs spectroscopy

Nanomaterials exhibit a variety of unusual and interesting optical properties that can differ significantly from the properties exhibited by the same bulk material. By carefully controlling the size, shape and surface functionality of nanoparticles a wide range of optical effects can generated with many useful applications. An optical response in a nanomaterial can be created through several different mechanisms, depending on the nanomaterial size, composition and arrangement, and each method may provide certain benefits depending on the target application.

The UV –Visible absorption spectroscopy is used to determine the optical properties of nanosized materials. The spectrum of $Zn^{+2}$ doped magnesium oxide nanoparticles NPs were recorded by Shimadzu Model No.1800 double beam U.V Spectrophotometer. The strong absorption peak at 354.09 nm obtained in UV-Vis absorption spectra having visible range between 200 to 800 nm wavelength, which confirmed the presence of zinc.

The UV-Vis absorption spectra of pure and $Zn^{+2}$ doped MgO NPs as a function of wavelength for the range of 200 to 800 nm Figure [ 3.5 (a,b) ]. It is noted that the absorption peak increases with the doping concentration. The strong absorbance is found for the wavelength below 354.09 nm for $Zn^{+2}$ doped MgO nanoparticles. This is attributed to greater absorption of incident photon energy by the molecules present in the lower energy state getting excited to the higher energy levels [24].The optical bandgap ($E_g$) is determined from a Tauc-plot). Absorption coefficient is define by following relation

$$\alpha = A(h\nu - E_g)^{1/2} h\nu$$

**Table-4.** Optical Band Gap for $Zn^{+2}$ doped MgO NPs duration of time

| Name of sample | Time duration of calcination | Band gap energy(eV) |
|---|---|---|
| $Zn^{+2}$ doped MgO NPS | 3 hrs (450 ˚C) | 3.1 eV |

Plots of $(\alpha h\nu)^2$ versus $(h\nu)$ are made for pure and $Zn^{+2}$ doped MgO NPs. The band gap energy ($E_g$) is obtained from the extrapolation of the linear portions of the plots onto the *x*-axis.

The band gap energy ($E_g$) for pure $Zn^{+2}$ doped MgO NPs is around 3.1 eV [ Table 4 & Fig 3.5 (c)] and decreases with $Zn^{+2}$ dopant [25].

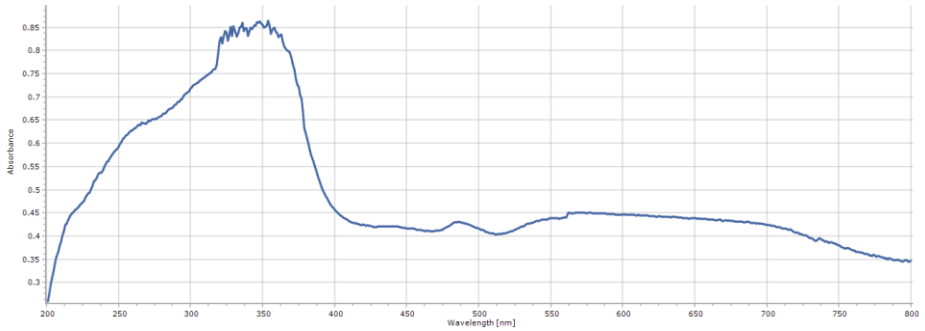


**Fig. 3.5 (a)** UV-Vis Absorption spectra

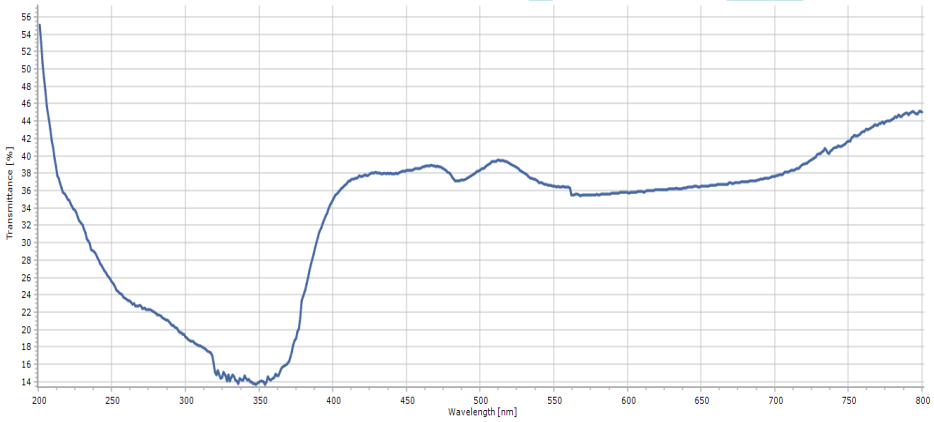


**Fig. 3.5(b)** UV-VIS Transmittance spectra

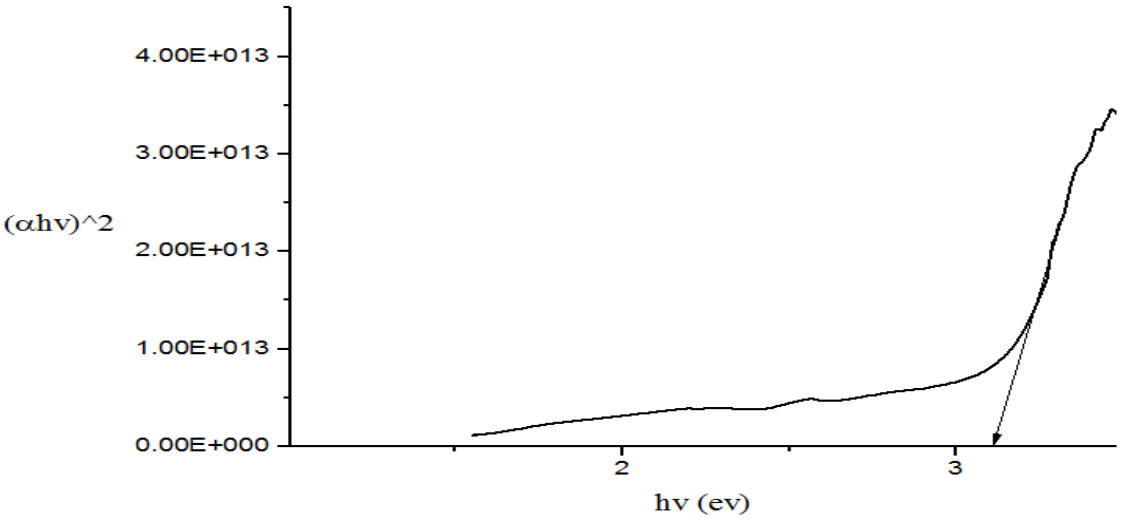


**Fig. 3.5 (c)** DRS graph of $Zn^{+2}$ doped MgO NPs

### 2.2.2.2- Photo luminance Analysis

Photoluminescence spectroscopy is a contactless, nondestructive method of probing the electronic structure of materials. The photo luminance spectroscopy is used to determine the impurities, structure and energy transfer. The PL spectra of $Zn^{+2}$ doped MgO nanoparticles was observed with the excitation wavelength of 335 nm as shown in the figure [3.6]. The PL spectrum gives the wide emission bands which are 378, 554, 595, 612 and 738 nm in 335 – 800 nm emission band range. The peak around 378 nm belongs to violet region, 554 nm belongs to green region and 595 nm belongs to orange region.

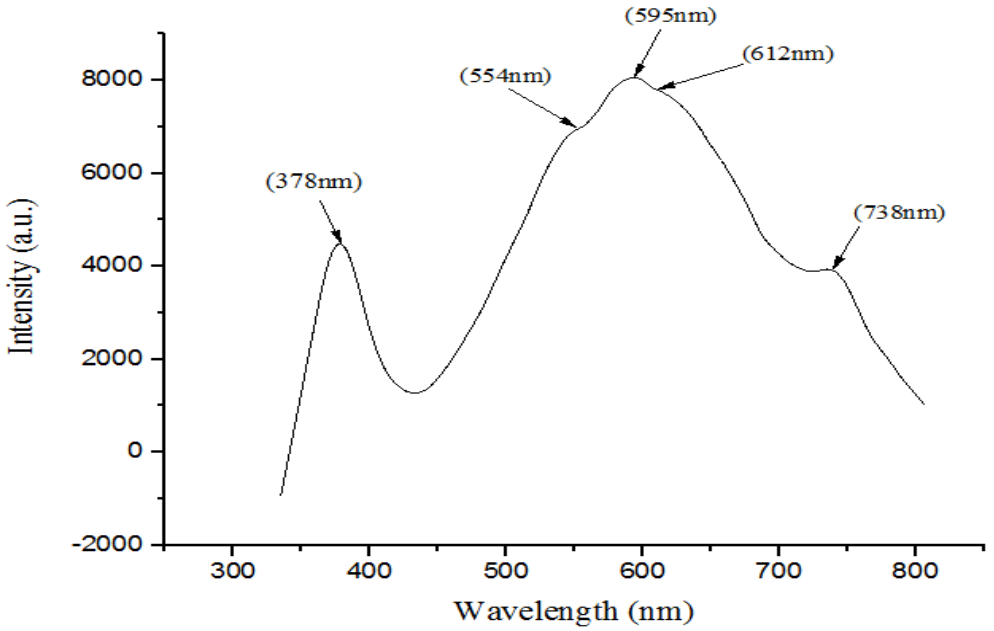


**Fig.3.6** Room temperature PL spectrum of Zn2+ doped MgO nanoparticles under the excitation wavelength of 335 nm.

The emission peak centered at 378 nm (violet region), 554nm (green region), 595nm (orange region) was attributed to surface defects namely oxygen vacancies, F-centres (oxygen ion vacancy occupied by two electrons) F+-centres (oxygen ion vacancy occupied by single electrons) surface states and 612nm and 738nm (red region) the red emission can be due to the relaxation luminescence of such defect centers created by mechanical stress during fracture and rapid crystallization [22]. The $Zn^{2+}$ doped MgO nanoparticles, in the present study, show two major bands in PL spectra at about 378 nm and 595 nm. The emission band at 378 nm is suppressed, whereas that at 595 nm is enhanced on increasing the concentration of $Zn^{2+}$.The $Zn^{2+}$ ions tend to segregate at low coordinated surface sites of MgO (edges and corners) which leads to decrease in the concentration of $Mg^{2+}$ ions on the surface and suppress the surface excitons due to MgO (378 nm). Solubility of $Zn^{2+}$ in MgO is temperature dependent as $Zn^{2+}$ has slightly larger ionic radius (0.74 A°) than that of $Mg^{2+}$ (0.72 A°). Similar photoluminescence spectral results have been reported by [23].

## 3- CONCLUSIONS

$Zn^{2+}$ doped MgO nanoparticles are prepared using green synthesis method at 60ºC temperature. Then, their properties were investigated by UV, FTIR, XRD, SEM, EDAX and PL, from XRD data the average grain size 44.75nm with $Zn^{2+}$

doped MgO. The maximum crystallite size obtained from XRD was less than 100nm. Indian ber and Jamun has works successfully as a catalyst and reducing agent and is rich of bio organic molecules as indicated by FTIR results. FTIR define all functional group in MgO nanoparticles. UV-Visible photo spectrometer within the range of 200–800 nm in which intense peak observed at 354.09 nm confirmed the formation of nanosized MgO particles. Optical band gap energy was found 3.10 eV with $Zn^{2+}$ doped MgO. SEM image of $Zn^{2+}$ doped MgO particles diameters of 20-70 nm. Energy dispersive X-ray spectroscopy (EDAX) define the presence of elemental metal signal (magnesium, zinc and oxygen) was confirmed. Photoluminescence spectra show emission bands due to the defects, and MgO-specific excitons. The $Zn^{2+}$ doped MgO nanoparticles with improved optical properties are expected to be useful in plasma display panels.

**ACKNOWLEDGEMENT:** - We are thankful to the Malaviya National Institute of Technology Jaipur, for providing the FTIR, PL, FE-SEM facilities and Banasthali University Newai, for providing the UV-Vis and XRD facilities.

**4- REFERENCES**

i. Ghashang, M., Mansoor, S.S.H., Shafiee, M.R.M., Kargar, M., Biregan, M.N., Azimi, F., and Taghrir, H., (2016) Green chemistry preparation of MgO nanopowders: efficient catalyst for the synthesis of thiochromeno[4,3-b]pyran and thiopyrano[4,3-b]pyran derivative, *J. Sulfur Chem.*, 37, 377-390.

ii. Huang, L., DQ, Li., YJ, Lin., Wei, M., Evans, DG., and Duan, X., (2005) Controllable preparation of Nano-MgO and investigation of its bactericidal properties, *J. Inorg. Bichem.*, 99, 986-993.

iii. Ouraipryvan, P., Sreethawong, T., and Chavadej, S., (2009) synthesis crystalline MgO nanoparticle with mesporous-assembled structure via a surfactant-modified sol-gel process, *Mater. Lett.*,63, 1862-1865.

iv. Esmaeili, E., Khodadadi, A., and Mortazavi, Y., (2009) Microwave-induced combustion process variables for MgO nanoparticle synthesis using polyethylene glycol and sorbitol, *J. Eur. Ceram. Soc.*,29, 1061-1068.

v. Stankic, S., Diwald, O., Sterrer, M., Knozinger, E., Hofmann, P., and Bernardi (2009) Novel optical surface properties of $Ca^{2+}$ -doped MgO nanocrystals, *J. Nano Lett.*, 5, 1889-1893.

vi. Yang, Q., Sha, J., Wang, L., Wang, J., and Yang, D., (2006) MgO nanostructures synthesized by thermal evaporation, *Mater. Sci. Eng.*, 26, 1097-1101.

vii. Yi, X., Wenzhong, W., Yitai, Q., Li., and Zhiwen. C., (1996) Deposition and microstructural characterization of MgO thin films by a spray pyrolysis method, C *Surf. Coat.Technol*., 82, 291-293.

viii. Phuoc, T.X., Howard, B.H., Martello, D.V., Soong, Y., and Chyu, M.K., *(*2008*)* Synthesis of $Mg(OH)_2$, MgO, and Mg nanoparticles using laser ablation of magnesium in water and solvents, *Opt. Lasers. Engg.*, 46, 829-834.

ix. Hao, Y., Meng, G., Ye, C., Zhang, X., and Zhang, L., (2005) Kinetics-driven growth of orthogonally branched single-crystalline magnesium oxide nanostructures, *J. Phys. Chem. B.*, 109, 11204-11208.

x. Kaviyarasu, K., and Devarajan, P.A., (2011) Synthesis and characterization studies of cadmium doped MgO nanocrystals for optoelectronics application, *Adv. Appl. Sci. Res.*, 2 131-138.

xi. Nair, R., Varghese, S. H., Nair, B.G., Maekawa, T., Yoshida, Y., and Kumar, S.D.,(*2010)* Nanoparticulate material delivery to plants, *Plant Sci.*, 179, 154-163.

xii. Vedpriya A. (2010), Living Systems: Eco-friendly nanofactories, *Dig. J. Nanomater. Biostruct.*, 5, 9-21.

xiii. Zak, A.K., Haliza, W., Majid, A., Abrishami, M.E.,and Yousefi (2011) X-ray analysis of ZnO nanoparticles by

Williamson–Hall and size–strain plot methods, *R.J. Solid State Sci*.,13, 251-256.
xiv. Swygenhoven., (2002) Grain Boundaries and Dislocations, *H.V. Science*, 296, 66-67.
xv. Greenwell, H.C., Jones, W., Stamires, D.N., Connor, P.O., and Brady M.F, (2006) A one-pot synthesis of hybrid organo-layered double ,hydroxide catalyst precursors, *Green Chem.*, 8, 1067-1072.
xvi. Shafee, M.R.M., and Karger M (2016) Preparation of aryl sulfonamides using CuO nanoparticles prepared in extractive Rosmarinus Officinalis leaves media Biointerface, *Res. Appl. Chem.*, 6, 1257-1262.
xvii. Kargar, M., Arani, S.A., Bagheri, S., and Niasari, M., (2014) Magnetic and structural characteristics of $HoBa_2Cu_3O_{7-x}$ nanorods synthesized in the presence of an appropriate surfactant, *M.S. Ceramics International*, 40, 11109-11114.
xviii. Lin, Z.D., Guo, F., Wang, C.,Wang, X., Wang, K., and Qu Y (2014) Preparation and sensing properties of hierarchical 3D assembled porous ZnO from zinc hydroxide carbonate , *RSC Adv.*, 4, 5122-5129.
xix. Etacheri, V., Roshan, R., and Kumar, V., (2012) Mg-Doped ZnO Nanoparticles for Efficient Sunlight-Driven Photo catalysis, *ACS Appl. Mater. Interfaces*, 4, 2717-2725.
xx. Azzaza, S., El-Hilo, M., Narayanan, S., Vijaya, J.J, Mamouni, N., Kenz, A., Bououdina, M., and Benyoussef, A., (2014) Structural, optical and magnetic characterizations of Mn-doped MgO nanoparticles, *J. Mater. Chem. Phys.*, 143, 1500-1507.
xxi. Sharrif, M.M., Verma, S.K., (2011) Aloe vera their chemicals composition and applications: A review, *Int. J. Biol. Med. Res.*, 2, 466-471.